An analysis of anisotropy of rocks containing shape fabrics of rigid inclusions

Nibir Mandal[a], Chandan Chakraborty[b,*], Susanta Kumar Samanta[a]

[a]*Department of Geological Sciences, Jadavpur University, Calcutta 700032, India*
[b]*Geological Studies Unit, Indian Statistical Institute, 203 B.T. Road, Calcutta 700035, India*

Received 12 August 1999; accepted 6 January 2000

Abstract

This paper presents a theoretical basis for estimation of mechanical anisotropy in homogeneous rocks containing shape fabrics of rigid inclusions. The analysis is based on two types of viscous models: one containing linear fabrics of prolate ($a > b = c$) inclusions (cf. *L*-tectonite) and the other containing planar fabrics of oblate ($a < b = c$) inclusions (cf. *S*-tectonite). Models show contrasting bulk viscosities in stretching (*normal viscosity*) and shearing (*shear viscosity*) parallel to the fabric. The axial ratio R ($= a/b$) and the volume concentration (ρ_v) of rigid inclusions appear to be the principal parameters in determining the viscosity contrast. In anisotropic models with linear fabrics, normal viscosity (η_p) increases monotonically with increase in R, whereas shear viscosity (η_s) increases to a maximum, and then drops down to a near-stationary value. In anisotropic models with planar fabrics, the normal viscosity increases little with increasing flatness of inclusions, but the variation assumes a steep gradient when the latter is large. Shear viscosity, on the other hand, is relatively less sensitive to the shape of inclusions. The ratio of normal and shear viscosities, conventionally described as *anisotropy factor* δ, in both the models is always greater than 1, indicating that normal viscosity will be essentially greater than shear viscosity, irrespective of the axial ratio of inclusions forming the fabric. Models with a linear fabric show contrasting normal viscosities in pure shear flow along and across the linear fabric. The anisotropy is expressed by the ratio of longitudinal and transverse normal viscosities (*anisotropic factor* σ). It is revealed that the transverse viscosity is essentially less than the longitudinal viscosity, as observed in test model

1. Introduction

Rocks may be mechanically anisotropic due to the presence of compositional layering or crystallographic and/or shape fabrics of the mineral grains. The rheological properties of such rocks are influenced by the mechanical anisotropy. It is, therefore, essential to establish the nature and degree of mechanical anisotropy in the rock to analyse its deformation behaviour and path (Weijermars, 1992). Multilayered rocks with layers of contrasting competence are the most well-studied anisotropic materials in relation to different deformation processes, such as folding under layer-parallel compression (Biot, 1965; Ramberg, 1964; Cobbold et al., 1971), boudinage under layer-normal compression (Strömgard, 1973), or partitioning of strain across layering (Treagus, 1988).

Viscosity of anisotropic rocks is a tensor quantity (Cobbold, 1976; Honda, 1986; Weijermars, 1992). Weijermars (1992) has shown that under layer-normal compression, the stiff layers in a multilayer govern the bulk viscosity (*normal viscosity*), which, under layer-parallel shear (*shear viscosity*), is controlled by the soft layers. The ratio of these two viscosities (anisotropic factor δ, Honda, 1986) is therefore, larger for larger viscosity contrast between the stiff and the soft units in the multilayer.

Studies on the mechanics of composite fibre structure have shown that the bulk strength of material depends greatly on the shape of stiff fibres (Cox, 1952; Kelly and Tyson, 1965, Laws and McLaughlin, 1978, Ting, 1999). This paper, following the above line of work, analyses the mechanical anisotropy of homogeneous rocks containing a linear or a planar fabric defined by preferred orientation of prolate and oblate rigid inclusions, respectively. The analysis takes into account the effects of shape and volume concentration of rigid inclusions on the *normal* (η_p) and *shear viscosities* (η_s) with respect to the fabric, and determines the anisotropic factor δ (η_p/η_s). An additional parameter, designated as the *anisotropic factor* σ, is introduced to describe the flow anisotropy in lineated rocks, which is the ratio of the viscosities in pure shear along (*longitudinal viscosity* η_{PL}) and across (*transverse viscosity* η_{PT}) the linear fabric (cf. Cobbold and Watkinson, 1981). The unequal flow in viscous models containing a linear fabric is tested with analogue model experiments.

2. Theoretical analysis

2.1. Anisotropic models

The mechanical models under consideration consist of spheroidal rigid inclusions in a homogeneous viscous matrix. We assume that the matrix is Newtonian viscous and the inclusions are non-clustering, non-interacting and randomly distributed, but with a preferred orientation, giving rise to a shape fabric in the bulk medium. The analysis is based on two types of mechanical models: (1) linear (cf. *L*-tectonite) and (2) planar (cf. *S*-tectonite) anisotropic models characterized by preferred orientation of prolate and oblate inclusions, respectively. The deformation considered is at constant volume.

2.2. Bulk viscosity of a medium

Consider a volume, *V*, in the homogeneous viscous

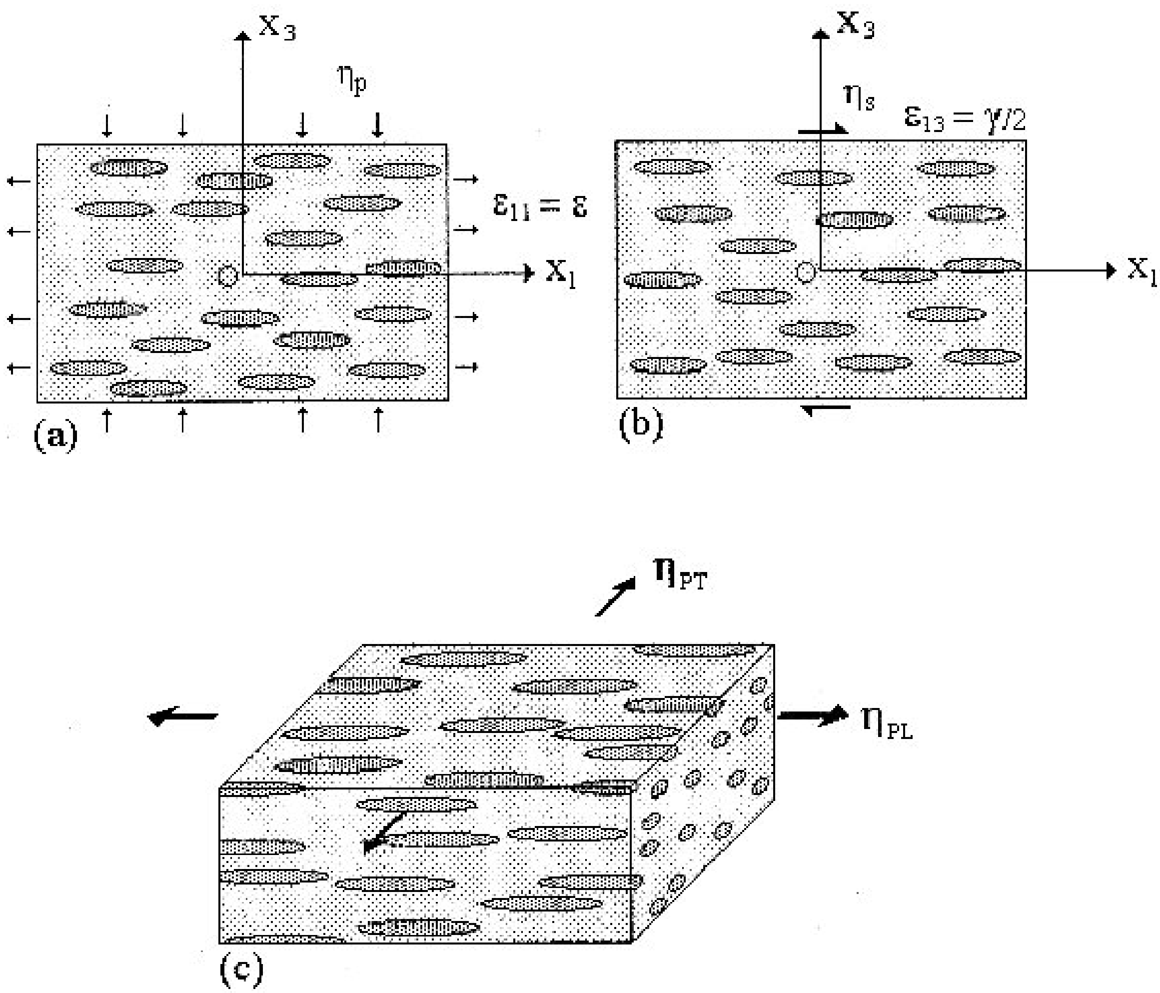

Fig. 1. Definitions of (a) normal viscosity η_p, (b) shear viscosity η_s and (c) longitudinal and transverse normal viscosities η_{PL}, η_{PT}.

medium, undergoing pure shear deformation at a strain rate, ε. The rate of work to be done for the deformation of the volume under consideration is:

$$\frac{dE}{dt} = 4\eta\varepsilon^2 V$$

(cf. equation 15(3) of Jaeger, 1969), where η is the coefficient of viscosity of the embedding medium. If the volume contains a rigid body, the mechanical interaction of the rigid body with the matrix would offer resistance to deformation for which an additional amount of work is to be done. In such a case, the total energy required for deformation per unit time is:

$$\frac{dE'}{dt} = \frac{dE}{dt} + \frac{dw}{dt} = 4\left(1 + \frac{V_P}{V}f\right)\eta\varepsilon^2 V \quad (1)$$

(cf. Jeffery, 1922), where V_p is the volume of the rigid body and f is a geometrical function. The bulk viscosity of the medium containing the rigid body can be written as: $\eta^* = (1 + \rho_v f)\eta$, where ρ_v is the volume fraction of rigid body (V_p/V) in the medium. The value of f is 5/2 (shown later), if the body is spherical in shape. The bulk viscosity of the medium then is $\eta^* = (1 + 2.5\rho_v)\eta$ (Einstein, 1911).

The bulk viscosity of the medium varies as the rigid body deviates from a spherical geometry (Jeffery, 1922). Moreover, the bulk viscosities would be different in different directions if there is a preferred orientation of rigid non-spherical inclusions in the matrix. The present analysis takes into consideration the two components of bulk viscosity tensor with respect to the fabric: *normal viscosity* and *shear viscosity* (Weijermars, 1992). Normal viscosity refers to the viscosity of the medium under pure shear with the principal axis of shortening perpendicular to the fabric and shear viscosity refers to that under shear parallel to the fabric, respectively (Fig. 1).

2.3. Normal viscosity and shear viscosity

Let us first consider that the anisotropic model is deformed by pure shear with the principal extension direction parallel to the a axis and no strain along the b direction of inclusions (Fig. 1a). It can be shown from Eq. (1) that the bulk viscosity of the medium under this kinematic state, i.e. normal viscosity, is:

$$\eta_p = \left[1 + \frac{1}{2}\frac{\rho_v}{ab^4}\frac{1}{\alpha_0'}\left(1 + \frac{\alpha_0''}{\beta_0''}\right)\right]\eta \quad (2)$$

where α_0', α_0'' and β_0'' are shape factors. The expressions of the shape factors and the derivation of Eq. (2) are given in Appendix A [Eqs. (A5a), (A5b) and (A8)]. It may be noted that $\alpha_0' = 2a^{-5}/5$ and $\alpha_0'' = \beta_0''$, if the inclusions are spherical in shape ($a = b$). The bulk viscosity in Eq. (2) is then $(1 + 2.5\rho_v)\eta$, as discussed in the earlier section. The normal bulk viscosity (η_p) in anisotropic models is obtained by substituting the expressions of α_0', α_0'' and β_0'' [Eqs. (A5a) and (A5b)] in Eq. (2). For convenience, we express the bulk viscosity as a dimensionless quantity (the ratio of bulk viscosity and matrix viscosity, η_p/η), in terms of the axial ratio of rigid inclusions ($R = a/b$).

In the linear anisotropic model:

$$\frac{\eta_p}{\eta} = 1 + \rho_v\frac{(1-R^2)^{\frac{5}{2}}}{R}\left[\frac{2}{2R\sqrt{R^2-1}(2R^2-5)+3\Omega} + \frac{1}{(2R^2+1)\Omega - 6R\sqrt{R^2-1}}\right] \quad (3a)$$

where $\Omega = \log[(R+\sqrt{R^2-1})/(R-\sqrt{R^2-1})]$

In the planar anisotropic model:

$$\frac{\eta_p}{\eta} = 1 + \rho_v\frac{(1-R^2)^{\frac{5}{2}}}{R}\left[\frac{2}{3\cos^{-1}R - R\sqrt{R^2-1}(5-2R^2)} + \frac{1}{(1+2R^2)\cos^{-1}R - 3R\sqrt{R^2-1}}\right]. \quad (3b)$$

We now consider that the anisotropic model is deformed by a fabric-parallel shear (Fig. 1b). Under this kinematic state, the bulk viscosity (i.e. shear viscosity) can be shown to have the expression:

$$\eta_s = \left[1 + \frac{2\rho_v}{ab^2(a^2+b^2)}\frac{1}{\beta_0'}\right]\eta \quad (4)$$

[see Eq. (A10) in Appendix A]. The shear viscosity in Eq. (4) is $(1+2.5\rho_v)\eta$ if the inclusions are spherical in shape [as $\beta_0' = 2a^{-5}/5$ for $a = b$ in Eq. (A4a)] as in case of pure shear. This implies that the bulk viscosity of a medium containing spherical inclusions will be same in coaxial (pure shear) and non-coaxial (simple shear) deformations. However, they will have different values when the inclusions are non-spherical. Substituting the expression of β_0' in Eq. (4), the dimensionless bulk shear viscosity ($\frac{\eta_s}{\eta}$) can be written as a function of the axial ratio ($R = a/b$) of inclusions.

For the linear anisotropic model:

$$\frac{\eta_s}{\eta} = 1 + 4\rho_v \frac{(R^2-1)^{\frac{5}{2}}}{R^2+1} \frac{1}{2(R^2+2)\sqrt{(R^2-1)} - 3R\Omega}. \quad (5a)$$

For the planar anisotropic model:

$$\frac{\eta_s}{\eta} = 1 + 4\rho_v \frac{(R^2-1)^{\frac{5}{2}}}{R^2+1} \frac{1}{(2+R^2)\sqrt{(1-R^2)} - 3R\cos^{-1}R}. \quad (5b)$$

The normalized bulk viscosity is essentially controlled by two dimensionless parameters: the axial ratio (R) and the volume concentration (ρ_v) of rigid inclusions. Eqs. (3a) and (5a) reveal that, in linear anisotropic models, with increase in elongation of rigid inclusions (i.e. increase in R) the normal viscosity generally increases with increasing gradients (Fig. 2a), whereas the shear viscosity increases to a maximum, and then decreases asymptotically down to a stationary value (Fig. 2b). In general, compared to normal viscosity, shear viscosity is much less sensitive to the axial ratio.

In planar anisotropic models, the normal viscosity increases little with increasing flatness (i.e. decreasing R) of inclusions [Eqs. (3b) and (5b)], but the variation assumes a steep gradient when the latter is high (Fig. 2c), giving rise to a large value of normal viscosity, e.g. $\eta_p/\eta = 25$ for $R = 0.01$ at $\rho_v = 0.4$. Shear viscosity is relatively less sensitive to the shape of inclusions. In contrast to normal viscosity, it shows an inverse variation with increasing flatness (Fig. 2d).

2.4. Anisotropic factor δ

It appears from Eqs. (3a), (3b), (5a) and (5b) that the degree of mechanical anisotropy, $\delta = \frac{\eta_p}{\eta_s}$, is greater than 1 for all values of R and ρ_v (Fig. 3) implying that the normal viscosity of an anisotropic body will be essentially greater than the shear viscosity, as in the case of multilayers (Weijermars, 1992).

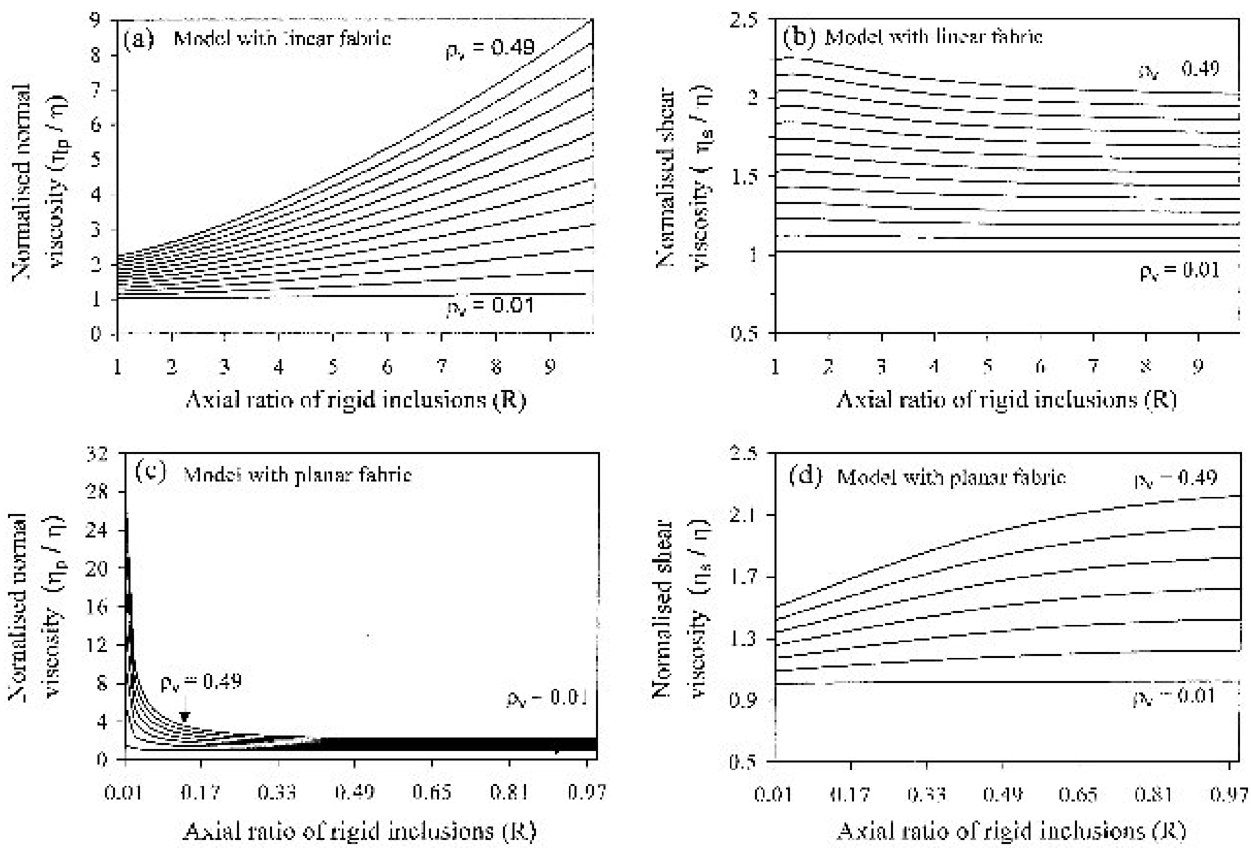

Fig. 2. Calculated plots of normal and shear viscosities η_p, η_s (normalized to matrix viscosity η) vs. axial ratio of inclusion R. (a) and (b) Anisotropic models with linear fabric. (c) and (d) Anisotropic models with planar fabric. The curves are drawn for values of volume concentration ρ_v at an interval of 0.04.

In linear anisotropic models, for a constant volume fraction ρ_v, with increase in axial ratio R (= a/b), δ increases with increasing gradients (Fig. 3a), whereas for a constant axial ratio, with the increase in volume concentration ρ_v, δ increases but with decreasing gradients (Fig. 3b). If the axial ratio of rigid inclusions is around 1.5, the anisotropic factor tends to be virtually insensitive to the volume concentration. Similarly, for low volume concentration of rigid inclusions, δ depends little on the axial ratio (Fig. 3a).

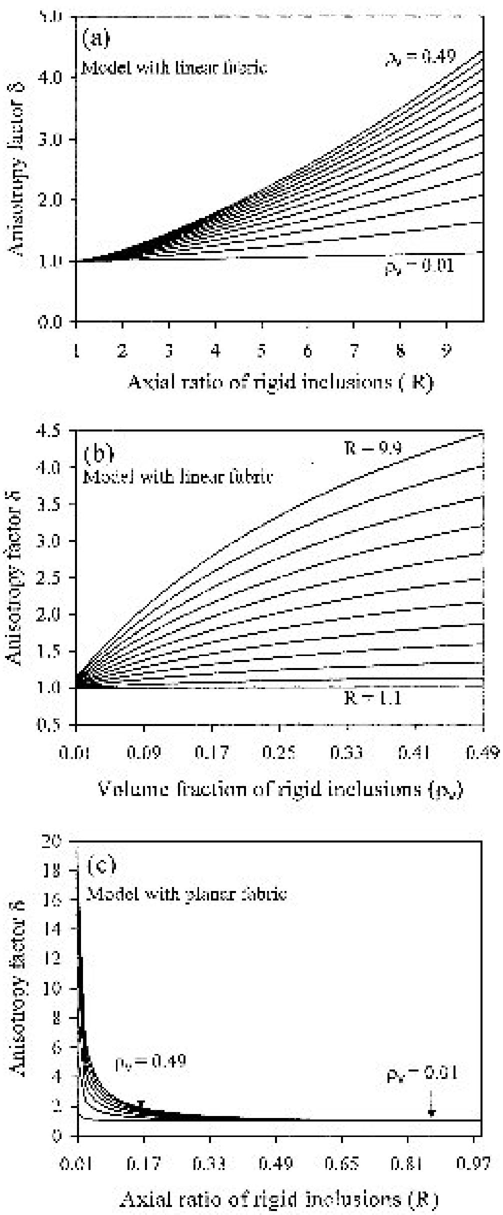

Fig. 3. (a) and (b) Variations of anisotropy factor δ with change in axial ratio of rigid inclusions R and volume concentration (ρ_v) in anisotropic model with linear fabric. Intervals of ρ_v and R are 0.04 and 0.8, respectively. (c) δ vs. R variations in anisotropic models with planar fabric. Interval of ρ_v = 0.08.

The factor δ for anisotropic models with a planar fabric is greater than 1 for all values of R and ρ_v, and its magnitude increases little with increasing flatness or decreasing axial ratio of the rigid inclusions, but jumps to large values at very low values of axial ratio (Fig. 3c).

2.5. Longitudinal and transverse normal viscosity

To find the longitudinal normal viscosity (η_{PL}) in anisotropic models with linear fabrics, consider a pure shear flow with the bulk extension parallel to the linear fabric, i.e. $\varepsilon_{11} = \varepsilon$, $\varepsilon_{33} = -\varepsilon$ and $\varepsilon_{12} = \varepsilon_{13} = \varepsilon_{23} = 0$ in Eq. (A3). Following the method adopted in the earlier cases, we have:

$$\eta_{PL} = \left[1 + \frac{\rho_v}{2}\left\{\frac{1}{ab^4}\frac{1}{\alpha_0'}\left(1 + \frac{\alpha_0''}{\beta_0''}\right)\right\}\right]\eta. \tag{6}$$

Eq. (6) shows that the bulk strength of a medium is greatly enhanced due to the presence of a fabric of elongate inclusions. With increase in axial ratio (R = a/b) of the inclusions, the longitudinal viscosity increases with increasing gradients (cf. Fig. 2a). The phenomenon is similar to the control exerted by the aspect ratio of fibres on the tensile strength of a fibre-reinforced metal (Kelly and Tyson, 1965).

Under the condition of bulk extension perpendicular to the linear fabric, [$\varepsilon_{11} = 0$, $\varepsilon_{22} = \varepsilon$, $\varepsilon_{33} = -\varepsilon$ and $\varepsilon_{12} = \varepsilon_{13} = \varepsilon_{23} = 0$ in Eq. (A3)], it can be shown from Eq. (A3) that the transverse normal viscosity has the expression:

$$\eta_{PT} = \left[1 + \frac{\rho_v}{ab^4}\frac{1}{\alpha_0'}\right]\eta. \tag{7}$$

It may be noted that, when $a = b$, Eqs. (6) and (7) become identical, as $\alpha_0'' = \beta_0''$, and give rise to an expression $(1 + 2.5\,\rho_v)\eta$ (as $\alpha_0' = 2/5\,a^{-5}$). For non-spherical shapes ($a \neq b$), $\alpha_0'' \neq \beta_0''$, and thereby, η_{PL} and η_{PT} have different values. The anisotropic factor ($\sigma = \frac{\eta_{PL}}{\eta_{PT}}$) can be written as:

$$\sigma = \frac{a^5\alpha_0' + \frac{1}{2}R^4\left(1 + \frac{\alpha_0''}{\beta_0''}\right)\rho_v}{a^5\alpha_0' + R^4\rho_v}. \tag{8}$$

In the model under consideration, $a > b$, $\alpha_0'' > \beta_0''$ [Eq. (A4b)]. The value of the factor σ in Eq. (8) is, therefore, greater than 1. The result suggests that the normal viscosity in the flow along a linear fabric is essentially greater than that across the fabric. The axial ratio (R) and the volume density (ρ_v) of prolate inclusions are the principal parameters in determining the degree of anisotropy. For a constant volume density of rigid inclusions, with increase in axial ratio of inclusions the anisotropic factor σ increases with increasing gradients (Fig. 4a). On the other hand, for a constant axial ratio, with increase in ρ_v the anisotropic factor increases, but lies within a limit (Fig. 4b), e.g. $\sigma < 3$ for $R = 6$. The factor σ does not vary significantly with the change in volume concentration when elongate inclusions have low axial ratios. It is, therefore, evident that a linear fabric of short grains cannot develop a strong mechanical anisotropy in the rocks even if the grains occupy a large volume proportion.

3. Discussion

The analysis reveals that in homogeneous rocks containing a shape fabric of rigid inclusions the normal viscosity is generally greater than the shear viscosity, as is the case with laminated orthotropic media (Weijermars, 1992). Whereas the ratio of normal and shear viscosities, i.e. the anisotropic factor δ (Honda, 1986), in laminated media shows a proportional relationship to the viscosity ratio of the stiff and the soft layers (Weijermars, 1992), that in media with a shape fabric is directly proportional to the axial ratio of the rigid inclusions. The fabric-controlled mechanical anisotropy can be large (say $\delta = 20$), as in the case of layered rocks, if the inclusions are extremely flat (with a/b ratio less than 0.01; Fig. 3c).

The volume concentration of rigid inclusions is another factor that controls the degree of anisotropy.

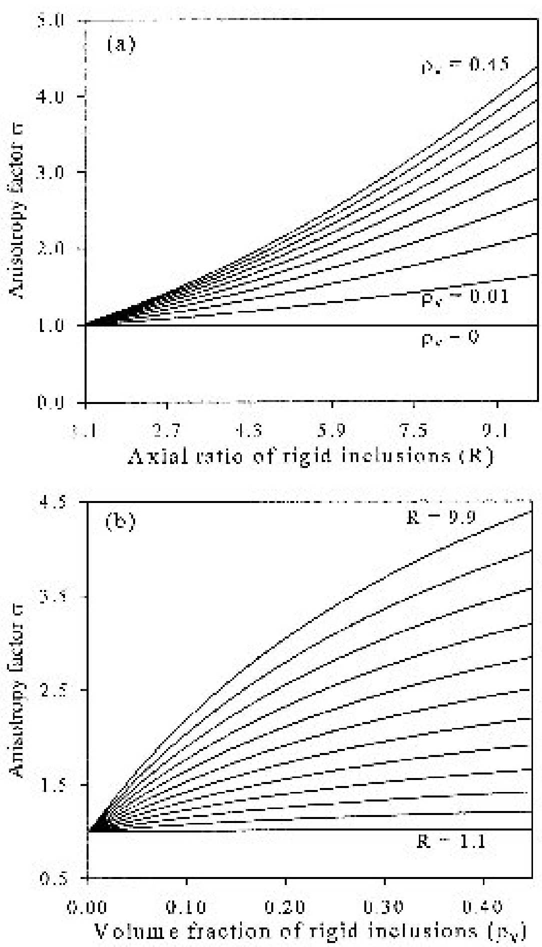

Fig. 4. (a) and (b) Variations of anisotropy factor σ with change in axial ratio of rigid inclusions R and volume concentration (ρ_v) in anisotropic model with linear fabric. Intervals of ρ_v and R are 0.06 and 0.8, respectively.

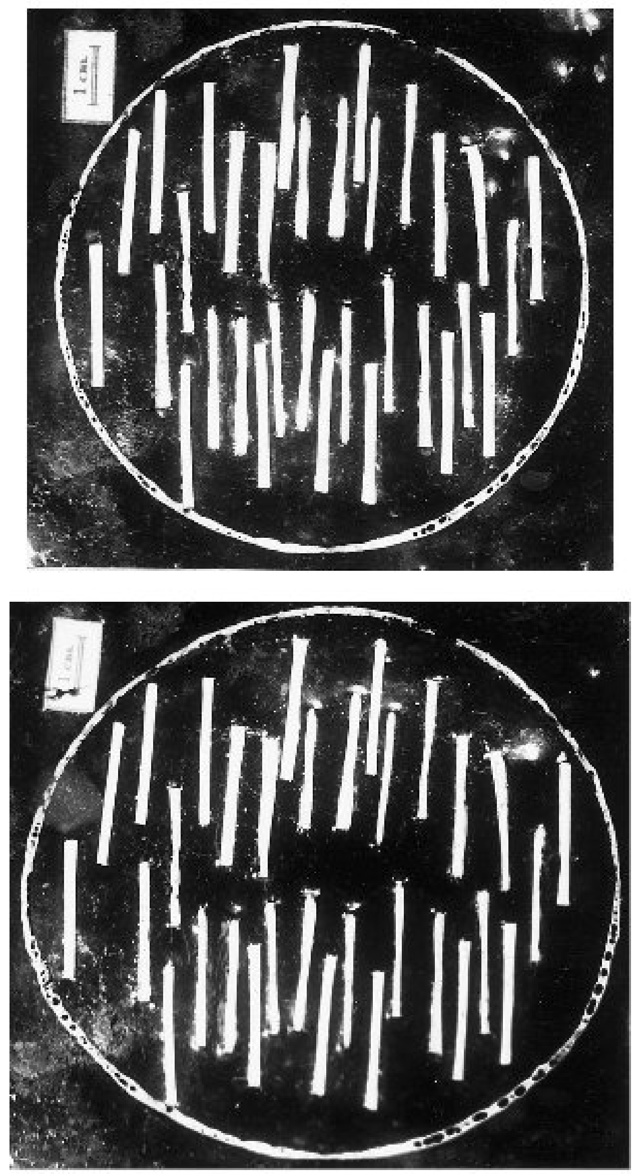

Fig. 5. Anisotropic flow in a pitch model containing a linear fabric of rigid inclusions. The axial ratio of individual inclusions is 15. The model flowed radially under its own weight. A passive marker represents the bulk strain in the model. This marker is circular in the initial state (top) and elliptical after deformation (bottom). Scale bar: 1 cm.

The mechanical anisotropy is apparently likely to be larger for larger volume concentration ρ_v. However, the analysis indicates that, for a given axial ratio of the inclusions, the degree of anisotropy does not increase linearly with increasing volume concentration, but tends to have a stationary value ($\delta \approx 3$, when $a/b = 6$).

The theoretical result that the viscosity in the bulk flow parallel to a linear fabric is greater than that across the fabric [Eq. (8)] has been tested with viscous pitch models. The viscosity of pitch was 1.5×10^6 Pa s at room temperature (30°C). The pitch block had oriented rigid sticks in a certain volume proportion. The top surface of the model was stamped with a circular mark encircling the portion containing rigid sticks. The model flowed laterally, and underwent flattening type of deformation under its own weight. The circular mark was deformed into an elliptical shape due to anisotropic flow. The long axis of the bulk-strain marker was at right angles to the linear fabric (Fig. 5), implying that the viscosity along the fabric is greater than that across the fabric. The axial ratio of the strain marker is a direct measure of the degree of anisotropy σ. For a volume fraction of 0.02 and an aspect ratio of rigid sticks of 15, the axial ratio of the strain marker was 1.2, which closely matches with the value of anisotropic factor obtained from Eq. (8).

In the course of deformation, prolate inclusions in a medium progressively get reoriented towards the bulk extension direction, eventually giving rise to a linear fabric. As a consequence, the bulk viscosity in the extension direction will increase in concert with fabric development. This implies that during progressive stretching the flow will experience more and more resistance along the extension direction, similar to work hardening in the direction of rolling of a metal sheet.

The limitations of the present model adhere to the assumptions that the embedding medium is Newtonian and there is no volume change. The model also assumes that the rigid inclusions are non-clustering and non-interacting. Understandably, such an assumption holds at lower volume concentration of rigid bodies in the matrix and the theory is likely to break down above a critical volume fraction.

Acknowledgements

We wish to thank Professor P. Cobbold and Dr. B Freeman for their critical reviews and suggestions for improvement of the manuscript. Dr. R.J. Lisle is specially thanked for giving us guidance for revising the manuscript. The present work has been supported by DST, India sanctioned to NM. CC acknowledges the infrastructural facilities provided by the Indian Statistical Institute.

Appendix A. General derivations

In this section we present the general mathematical derivations that have been utilized for the analysis of viscosity under specific kinematic conditions in the main text. The mathematical formulation is entirely based on Jeffery's (1922) theory on the mechanics of fluid containing ellipsoidal rigid inclusions.

Let us consider an infinitely extended viscous medium of viscosity η, containing spheroidal rigid inclusions of identical shape and orientation. Let the axial dimensions of individual inclusions be a, b and c. Models with planar fabric have inclusions of dimensions $a < b = c$, whereas those with linear fabric have inclusions with dimensions $a > b = c$. A Cartesian co-ordinate (x_1, x_2, x_3) is chosen with x_1 and x_3 axes parallel to a and c axial directions, respectively (Fig. 1). With respect to this co-ordinate system, the kinematic state of the bulk medium is represented by a velocity gradient tensor:

$$L_{ij} = \begin{bmatrix} \varepsilon_{11} & \varepsilon_{12} & \varepsilon_{13} \\ \varepsilon_{12} & \varepsilon_{22} & \varepsilon_{23} \\ \varepsilon_{13} & \varepsilon_{23} & \varepsilon_{33} \end{bmatrix} + \begin{bmatrix} 0 & \omega_{12} & \omega_{13} \\ \omega_{12} & 0 & \omega_{23} \\ \omega_{13} & \omega_{23} & 0 \end{bmatrix}. \tag{A1}$$

The first and second terms in Eq. (A1) are the distortion and rotation (spin) tensors, respectively. The rotation tensor will not contribute to the work done during deformation and only the six strain rate components in the distortion tensor are significant. Of these six strain rates, five are independent because there are no volume changes in the present model. Let us take a volume, V, in the medium, which is much larger in size compared to individual inclusions. There are n inclusions within the volume under consideration. The energy required per unit time for the deformation of the volume is:

$$\frac{dE'}{dt} = 2V\eta\left(\varepsilon_{11}^2 + \varepsilon_{22}^2 + \varepsilon_{33}^2 + 2\varepsilon_{12}^2 + 2\varepsilon_{23}^2 + 2\varepsilon_{13}^2\right) + \frac{32}{3}\pi n\eta(A\varepsilon_{11} + B\varepsilon_{22} + C\varepsilon_{33} + 2D\varepsilon_{12} + 2E\varepsilon_{13} + 2F\varepsilon_{23}) \tag{A2}$$

(Jeffery, 1922). The second part in Eq. (A2) represents the rate of additional energy to be spent due to the presence of rigid inclusions, where A, B, C … are constants that depend on the axial dimensions of individual inclusions and the components of bulk strain-rate tensor, and can be expressed as (equation 60 of Jeffery, 1922):

$$\frac{dw}{dt} = \frac{16}{3}\pi n\eta\left\{\frac{1}{2b^2\alpha_0'}\left(\varepsilon_{33}^2+\varepsilon_{22}^2+\frac{\alpha_0''}{\beta_0'}\varepsilon_{11}^2\right) + 2\left(\frac{\varepsilon_{12}^2+\varepsilon_{13}^2}{\beta_0'(a^2+b^2)}+\frac{\varepsilon_{23}^2}{2b^2\alpha_0'}\right)\right\} \quad \text{(A3)}$$

where α_0', β_0' and α_0'', β_0'' are geometrical parameters. After equations (10) of Jeffery, 1922, they can be expressed by integral functions as:

$$\alpha_0' = \int_0^\infty \frac{d\lambda}{(b^2+\lambda)^3(a^2+\lambda)^{\frac{1}{2}}},\ \beta_0' = \int_0^\infty \frac{d\lambda}{(b^2+\lambda)^2(a^2+\lambda)^{\frac{3}{2}}} \quad \text{(A4a)}$$

and

$$\alpha_0'' = \int_0^\infty \frac{\lambda d\lambda}{(b^2+\lambda)^3(a^2+\lambda)^{\frac{1}{2}}},\ \beta_0'' = \int_0^\infty \frac{\lambda d\lambda}{(b^2+\lambda)^2(a^2+\lambda)^{\frac{3}{2}}} \quad \text{(A4b)}$$

where λ is the ellipsoidal co-ordinate of a point with respect to the centre of an inclusion. The solutions of Eqs. (A4a) and (A4b) are as follows: when $a > b$,

$$\alpha_0' = \frac{1}{a^5}\frac{R^4}{4(R^2-1)^2}\left\{(2R^2-5)R^2 + \frac{3}{2}\frac{R}{\sqrt{R^2-1}}\log\left(\frac{R+\sqrt{R^2-1}}{R-\sqrt{R^2-1}}\right)\right\}$$

$$\beta_0' = \frac{1}{a^5}\frac{R^4}{(R^2-1)^2}\left\{2+R^2 - \frac{3}{2}\frac{R}{\sqrt{R^2-1}}\log\left(\frac{R+\sqrt{R^2-1}}{R-\sqrt{R^2-1}}\right)\right\}$$

$$\alpha_0'' = \frac{1}{a^3}\left[\frac{3}{2R^4}+\frac{R^4(2R^2-5)}{4(R^2-1)^2} + \frac{1}{2\sqrt{R^2-1}}\left(\frac{3R^3}{2(R^2-1)^2} - \frac{2R^2+1}{2R^5}\right)\log\frac{R+\sqrt{R^2-1}}{R-\sqrt{R^2-1}}\right] \quad \text{(A5a)}$$

$$\beta_0'' = \frac{1}{a^3}\frac{1}{2R^5\sqrt{R^2-1}}\left\{(2R^2+1)\log\left(\frac{R+\sqrt{R^2-1}}{R-\sqrt{R^2-1}}\right) - 6R\sqrt{R^2-1}\right\}$$

and when $a < b$,

$$\alpha_0' = \frac{1}{b^5}\frac{1}{4(1-R^2)^{\frac{5}{2}}}\left\{3\tan^{-1}\frac{\sqrt{1-R^2}}{R} - R\sqrt{1-R^2}(5-2R^2)\right\}$$

$$\beta_0' = \frac{1}{b^5}\frac{1}{R(1-R^2)^{\frac{5}{2}}}\left\{(2+R^2)\sqrt{1-R^2} - 3R\tan^{-1}\frac{\sqrt{1-R^2}}{R}\right\}$$

$$\alpha_0'' = \frac{1}{b^3}\frac{1}{4(1-R^2)^{\frac{5}{2}}}\left\{(1-4R^2)\tan^{-1}\frac{\sqrt{1-R^2}}{R} + R(1-R^2)(1+2R^2)\right\} \quad \text{(A5b)}$$

$$\beta_0'' = \frac{1}{b^3}\frac{1}{(1-R^2)^{\frac{5}{2}}}\left\{(1+2R^2)\tan^{-1}\frac{\sqrt{1-R^2}}{R} - 3R\sqrt{1-R^2}\right\}.$$

R is the axial ratio (a/b) of rigid inclusions. It may be noted that these equations are comparable to equations (67) and (68) of Jeffery (1922). Eqs. (A3), (A5a) and (A5b) indicate that the shape of rigid inclusions and the strain-rate components control the rate of additional work and thereby, the bulk viscosity of the medium, as in Eq. (1).

Normal viscosity

If ε is the rate of pure shear flow with principal extension along a axial direction, then $\varepsilon_{11} = \varepsilon$, $\varepsilon_{33} = -\varepsilon$, $\varepsilon_{12} = \varepsilon_{13} = \varepsilon_{23} = 0$. It can be shown that the expression for the rate of additional work in Eq. (A3) is:

$$\frac{dw}{dt} = \frac{8}{3}\pi n\eta\frac{1}{b^2}\left[\frac{\alpha_0''}{\alpha_0'\beta_0''}+\frac{1}{\alpha_0'}\right]\varepsilon^2,$$

which can be rearranged as:

$$\frac{dw}{dt} = 2V_p n\eta\left[\frac{1}{ab^4}\left(\frac{\alpha_0''}{\alpha_0'\beta_0'}+\frac{1}{\alpha_0'}\right)\right]\varepsilon^2$$

where V_p is the volume of individual inclusions. From Eq. (1), the rate of total work done is:

$$\frac{dE'}{dt} = 4V\eta\varepsilon^2\left[1+\frac{1}{2}\rho_v\frac{1}{ab^4}\left\{\frac{1}{\alpha_0'}\left(1+\frac{\alpha_0''}{\beta_0''}\right)\right\}\right]. \quad \text{(A6)}$$

If the bulk viscosity is represented by η_p, the rate of work done for the flow in the volume, V, is:

$$\frac{dE'}{dt} = 4V\eta_P\varepsilon^2. \tag{A7}$$

Comparing Eqs. (A6) and (A7), we have the expression of normal viscosity:

$$\eta_P = \left[1 + \frac{1}{2}\frac{\rho_v}{ab^4}\frac{1}{\alpha_0'}\left(1 + \frac{\alpha_0''}{\beta_0''}\right)\right]\eta. \tag{A8}$$

Shear viscosity

Let us now consider a simple shear flow parallel to the fabric at a rate γ (Fig. 1b). Then, $\varepsilon_{13} = \gamma/2$, and all other strain-rate components in Eq. (A1) are zero. Under this kinematic condition,

$$\frac{dw}{dt} = \frac{16}{3}\pi n\eta\left[\frac{\gamma^2}{2\beta_0'(a^2 + b^2)}\right].$$

The total strain energy in the deformation of volume, V, is

$$\frac{dE'}{dt} = \eta V\gamma^2 + \frac{2\rho_v V}{ab^2}\left[\frac{1}{\beta_0'(a^2 + b^2)}\right]\eta\gamma^2. \tag{A9}$$

Comparing Eqs. (A7) and (A9), the expression of shear viscosity follows:

$$\eta_s = \left[1 + \frac{2\rho_v}{ab^2(a^2 + b^2)}\frac{1}{\beta_0'}\right]\eta. \tag{A10}$$

References

Biot, M.A., 1965. Mechanics of Incremental Deformations. John Wiley and Sons, New York.

Cobbold, P.R., Cosgrove, J.W., Summers, J.M., 1971. Development of internal structures in deformed anisotropic rocks. Tectonophysics 12, 23–53.

Cobbold, P.R., 1976. Mechanical effects of anisotropy during large finite deformations. Bulletin of Geological Society of France 18, 1497–1510.

Cobbold, P.R., Watkinson, A.J., 1981. Bending anisotropy: a mechanical constraint on the orientation of fold axes in an anisotropic medium. Tectonophysics 72, T1–T10.

Cox, H.L., 1952. The elasticity and strength of paper and other fibrous materials. British Journal of Applied Physics 3, 72–79.

Einstein, A., 1911. Eine neue Bestimmung der Molekuldimensionen. Annalen Der Physik 34, 591.

Honda, S., 1986. Strong anisotropic flow in a finely layered asthenosphere. Geophysical Research Letters 13, 1454–1457.

Jaeger, J.C., 1969. Elasticity, Fracture and Flow. Methuen, London.

Jeffery, G.B., 1922. The motion of ellipsoidal particles immersed in a viscous fluid. Proceedings of the Royal Society of London A 120, 161–179.

Kelly, A., Tyson, W.R., 1965. Tensile properties of fibre-reinforced metals: copper/tungsten and copper/molybdenum. Journal of Mechanics and Physics of Solids 13, 329–350.

Laws, N., McLaughlin, R., 1978. The effect of fibre length on the overall moduli of composite materials. Journal of Mechanics and Physics of Solids 27, 1–13.

Ramberg, H., 1964. Selective buckling of composite layers with contrasted rheological properties, a theory for the formation of several orders of folds. Tectonophysics 1, 307–341.

Strömgard, K.E., 1973. Stress distribution during formation of boudinage and pressure shadows. Tectonophysics 16, 215–248.

Ting, J.-M., 1999. Tensile properties of VGCF reinforced carbon composites. Journal of Material Science 34, 229–233.

Treagus, S.H., 1988. Strain refraction in layered systems. Journal of Structural Geology 10, 517–527.

Weijermars, R., 1992. Progressive deformation in anisotropic rocks. Journal of Structural Geology 14, 723–742.